Published in final edited form as:
Heart Rhythm. 2014 March ; 11(3): 492–501. doi:10.1016/j.hrthm.2013.11.026.

Selective Inhibition of Late Sodium Current Suppresses Ventricular Tachycardia and Fibrillation in Intact Rat Hearts

Arash Pezhouman, MD[1], **Sepideh Madahian, MD**[1], **Hayk Stepanyan, BS**[1], **Hayk Ghukasyan, BS**[1], **Zhilin Qu**[1], **Luiz Belardinelli, MD**[2], and **Hrayr S. Karagueuzian, PhD, FHRS**[1]

[1]Translational Arrhythmia Research Section, UCLA Cardiovascular Research Laboratory, Department of Medicine Division of Cardiology, David Geffen School of Medicine at UCLA, Los Angeles, California

[2]Gilead Sciences Inc., Foster City, California

Abstract

Background—Enhanced late inward Na current (I_{Na-L}) modulates action potential duration (APD) and plays a key role in the genesis of early and delayed afterdepolarizations (EADs & DADs) and triggered activity.

Objectives—To define the influence of selective block of the I_{Na-L} on EAD- & DAD-mediated triggered ventricular tachycardia and fibrillation (VT & VF) in intact hearts using (GS967), a selective and potent (IC_{50}=0.13±0.01 μM) blocker of the I_{Na-L}.

Methods—VT/VF were induced either by local aconitine injection (50 μg) in the LV muscle of adult (3–4 months) male rats (N=21) or by arterial perfusion of 0.1 mM H_2O_2 in aged male rats (24–26 months, N=16). The LV epicardial surface of the isolated-perfused hearts was optically mapped using fluorescent voltage-sensitive dye, and microelectrode recordings of APs were made adjacent to the aconitine injection site. The suppressive and preventive effects of GS967 (1 μM) against EAD/DAD-mediated VT/VF were then determined.

Results—Aconitine induced VT in all 13 hearts studied. Activation map (N=6) showed that the VT was initiated by a focal activity arising from the aconitine injection site (CLs of 84±12) that degenerated to VF (CL=52±8 ms) within a few seconds. VF was maintained by multifocal activity with occasional incomplete reentrant wavefronts. Administration of GS967 suppressed the VT/VF in 10 out of 13 hearts (P<0.001). Pre-exposure to GS967 for 15 min prior to aconitine injection prevented the initiation of VT/VF in 5 of 8 additional hearts (P<0.02). The VF reoccurred within 10 min upon washout of GS967. Microelectrode recordings (N=7) showed that the VT/VF was initiated by EAD- and DAD-mediated triggered activity at CL of 86±14ms (NS from VT CL) that preceded the VF. GS967 shortened the AP duration (APD), flattened the slope of the dynamic APD restitution curve and reduced APD dispersion from 42±12 ms to 8±3 ms (P<0.01). H_2O_2

Corresponding author: Hrayr S. Karagueuzian, PhD, FHRS, FACC, Professor of Medicine & Director, Translational Arrhythmia Research Section, Cardiovascular Research Laboratory, David Geffen School of Medicine at UCLA, 675 Charles E. Young Dr. South, MRL 1630, Mail Code: 176022, Los Angeles, CA 90095, 310-825-9360 (phone), 310-206-5777 (fax), hkaragueuzian@mednet.ucla.edu.

Conflict of interest statement:
LB is an employee of Gilead Sciences Inc. and HSK is a recipient of unrestricted research award from Gilead.

perfusion in 8 fibrotic aged hearts promoted EAD-mediated focal VT/VF, which was suppressed by GS967 in 5 hearts ($P<0.02$).

Conclusions—The selective I_{Na-L} blocker GS967 effectively suppresses and prevents aconitine and oxidative stress-induced EADs, DADs and focal VT/VF. The suppression of EADs, DADs and reduction of APD dispersion make GS967 a potentially useful antiarrhythmic drug in conditions of enhanced I_{Na-L}.

Keywords

Optical mapping; late INa; aconitine; oxidative stress; ventricular tachyacrdia; ventricular fibrillation; early and late afterdepolairzations

Introduction

An emerging new strategy to suppress the initiation of triggered ventricular tachycardia and ventricular fibrillation (VT & VF respectively) is to prevent pathological increases in the late inward Na current (I_{Na-L}).[1–4] Enhanced I_{Na-L} seen in human heart failure,[5, 6] patients with LQT3 syndrome[7] and in diverse animal models including aconitine[8, 9] and oxidative stress[10, 11] plays an important role in promoting early and delayed afterdepolarizations (EAD & DAD respectively).[12] These afterpotentials initiate triggered activity[1, 2, 12–14] that may cause focal VT[15, 16] and VF[17] maintained by multifocal mechanisms.[2, 18] Previous studies have shown that the inhibition of the I_{Na-L} with sodium channel blocking drugs like ranolazine, flecainide and mexiletine suppresses EAD- and DAD-mediated triggered arrhythmias.[1, 2, 19] However, none of these drugs are sufficiently selective inhibitors of the I_{Na-L} including ranolazine, as they also affect the conductances of other ion channels. As a result the exclusive role played by the enhanced I_{Na-L} in the genesis of focal VT and multifocal VF in intact hearts remains unclear. The recent synthesis of a highly selective and potent (IC_{50}= 0.13 μM) blocker of the I_{Na-L}, GS-458967 (GS967), that completely eliminates the I_{Na-L}, while having minimal or no effect on the conductances of other ion channels,[1, 20] made the study of the exclusive role of the enhanced I_{Na-L} in the genesis of focal VT/VF possible. The Table, modified from ref. #1, describes the comparative potencies of GS967 against I_{Na-L} relative to ranolazine and flecainide. In this study we hypothesize that focal EAD/DAD-mediated VT/VF associated with aconitine and oxidative stress is suppressed by selective inhibition of the I_{Na-L} with GS967. Preliminary data have been reported in an abstract form.[21]

Methods & Materials

Surgical preparation and electrophysiological recordings

We studied 21 adult (~3 months) and 16 aged (23–25 months) male Fisher344 rats. This investigation conforms to the Guide for Care and Use of Laboratory Animals published by the National Institutes of Health (NIH PublicationNo.85-23, revised1996) and was approved by the Animal Research Committee of the UCLA. The hearts of the anesthetized rats were removed and cannulated and perfused through the aorta at 5 ml/min in a Langendorff setting. Simultaneous ECG, ventricular and atrial electrograms and single cell glass microelectrode recordings of transmembrane action potential (AP) were made from the left ventricular (LV) epicardium. To enhance the I_{Na-L} and EAD/DAD-mediated VT/VF, we injected 50 μg aconitine directly into the LV muscle at a lateral LV site midway between the base and the apex and made microelectrode recordings within 1 mm of the aconitine injection site towards the base of the LV. In the oxidative stress model, H_2O_2 (0.1 mM) was perfused arterially in the aged fibrotic hearts shown previously by us to manifest oxidative stress-mediated EADs and VT/VF.[2, 18, 22]

Optical mapping of activation

The LV epicardial activation pattern during the sinus rhythm and the onset of the VT and VF were mapped using voltage sensitive fluorescent dye (RH-237) in both models as we described previously.[2, 23] We evaluated the suppressive and the preventive effects of GS967 against the aconitine- and H_2O_2-induced VT/VF models using 1 μM GS967 delivered via arterial perfusion. For the suppressive protocol, GS967 was perfused within two minutes after the onset of VT/VF and for the preventive protocol, GS967 was perfused 15 min prior to the application of either aconitine or H_2O_2. We also determined the effect of aconitine and GS967 on the dynamic APD restitution curve as described previously.[2]

Histological analyses

Percent tissue fibrosis of the ventricles in the aged hearts was determined from 5-μm-thick histological sections stained by Masson's trichrome as previously described.[22]

Statistical analyses

Significant differences in the incidence of VT/VF (dichotomous comparisons) were determined using Fisher's exact test. Repeated measures ANOVA were done to determine changes of AP parameters.[23] We considered P values of ≤ 0.05 as significant and all data are presented as means ±SD.

Results

Activation maps during aconitine-induced VT

Figure 1 shows the electrical propagation pattern in an adult isolated heart during sinus rhythm. No conduction slowing and or block developed. After local injection of aconitine, monomorphic VT at a mean cycle length (CL) of 84±12 ms (N=13) arose as shown in Figure 2. We optically mapped six hearts to study the mechanism of VT onset. The VT in all these studies originated from focal activation from the near aconitine injection site and propagated over the entire mapped left ventricular (LV) surface. This pattern of activation is consistent with our previous mapping studies with aconitine in isolated swine ventricles.[16] The focal monomorphic VT lasted 4±1 sec before degenerating to VF which was maintained by multiple independent foci at a mean CL of 52±8 ms as shown in Figure 3. Occasionally incomplete reentrant wavefronts emerged during VF that propagated between the foci before dying out. In 2 out of 13 hearts, VT remained sustained and did not degenerate to VF. The optical action potentials (AP) during the focal VT and multifocal VF suggested the presence of EADs and DADs as indicated by the arrows in Figures 2 & 3.

Microelectrode recordings of aconitine-induced VT/VF

In order to provide evidence for the presence of EADs and DADs, we used continuous microelectrode recordings within 1 mm of the local aconitine injection site in 8 hearts to capture the onset of the VT. Figure 4 illustrates an example of simultaneous ECG and microelectrode recordings at the onset of aconitine-induced VT followed by VF. Both DADs and EADs were present prior to the initiation of VT. As shown in Fig 4A, the fourth beat of sinus origin manifested as an AP with an EAD (AP #4) is followed by a DAD-mediated triggered beat (beat labeled ES, extrasystolic beat and shown as a premature ventricular complex (PVC) on the pseudo-ECG. The ES beat was then followed by a sub-threshold DAD (<5 mV) as was the next 5^{th} beat of sinus origin (Fig 4A). The sixth sinus beat, however, suddenly gave rise to an AP and a late EAD-induced triggered activity initiating a monomorphic VT as shown on the ECG (Fig 4A). The mean CL of the triggered activity (86±14 ms) was no significantly different from the CL of the monomorphic VT (84±12 ms). The VT was then maintained by both EADs and DADs as shown during faster sweep

microelectrode recordings in Fig 4B. The monomorphic VT degenerated to VF within 4 sec as shown in Figure 4A. The occurrence of DADs following a previous AP with and EAD can be seen more clearly at faster sweep speed as shown in Figure 4B and is consistent with previous findings.[24] Thus, it appears that a direct synergism exists between EADs & DADs, as EAD's promote DADs and DAD-induced triggered activity. The aconitine-induced VF, if left uninterrupted, could last for >30 min period that we monitored (N=5) and could not be terminated with electrical shocks. The VF reemerged immediately after the application of multiple shocks.

Comparative efficacy of GS967 relative to ranolazine and flecainide

The Table shows that the IC50 value of GS967 to block the late INa is 26 and 130 smaller (more potent) than the IC50 values for flecainide and ranolazine respectively. GS967 causes no block of peak INa and IKr unless its concentration is raised to 10 μM (i.e., 10 times higher than the concentration used in this study) at which point only 7.5% and 17% reduction in peak INa and IKr develops respectively.

Suppressive Effect of GS967 Against Aconitine-Induced VT/VF

GS967 (1 μM) suppressed aconitine-induced VF in 10 out 13 hearts studied ($P<0.01$) within a mean of 7±4 min, as illustrated in Figure 5. The termination of the VF was associated with progressive suppression of the EADs/DADs and shortening of the APD as shown in Figure 5B & C. In the remaining four hearts short runs of monomorphic VT (N=3 hearts) and sustained monomorphic VT (one heart) persisted after GS967. The suppressant effect of GS967 against aconitine-induced VT/VF was reversible. Washout of the GS967 caused reemergence of the VT/VF within 8 min (mean of 7±4 min, N=5), as shown in Figure 5D, which was suppressed again when the heart was perfused a second-time with GS967, as shown in Figure 5E. It is interesting to note that the restoration of sinus rhythm after the termination of VF with GS967 is first preceded by the emergence of a VT then sinus rhythm with considerable shortening of the APD. (Figure 5B & 5E) This dynamic sequence of events is just the reverse of the sequence aconitine induced VF which first starts with the conversion of sinus rhythm to VT, which then degenerates to VF.

Preventive effect of GS967 against aconitine-induced VT/VF

The preventive efficacy of GS967 against aconitine-induced VT/VF was tested by arterial perfusion of GS967 starting 15 minutes before aconitine injection. Prophylactic perfusion of GS967 prevented VT/VF initiation in 5 out 8 hearts ($P<0.03$) studied for up to one hour of combined GS967 and aconitine administrations. In the remaining two hearts, short runs of VF and VT were observed during the 60 minutes of combined drug administration. Washout of GS967 caused the emergence of VT/VF in the 5 out of the 8 hearts studied within 10 min of washout of GS967.

Effect of GS967 on maximum APD dispersion, use-dependency & restitution

Maximum APD dispersion was determined by subtracting the longest APD from the shortest APD over the entire LV epicardial surface. During sinus rhythm, with a mean CL of 235±55 ms, GS967 reduced the maximum APD dispersion from 42±12 ms to 8±3 ms, $P<0.01$. The dispersion during VT at a mean CL of 86±10 ms just prior to conversion to sinus rhythm was 20±6 ms as shown in Figure 6. Conduction velocity remained unchanged under all conditions as the entire LV epicardium was activated with 12 ms as shown in the isochronal maps of Figure 6. GS967 induced shortening of the APD from 76±11 ms to 36±6 ms ($P<0.01$) during pacing at a CL of 250 ms (5 hearts & 28 cells). The shortening of the APD by GS967 was use-dependent, with greater APD shortening occurred with decreasing the pacing CL (7A–D). In contrast, GS967 has little effect on the AP amplitude (APA), except

for a slight (7%) but significant reduction at PCLs <200 ms (P<0.05) as shown in Figure 7D. Together with the lack of conduction slowing effect of GS967 (Figure 6), these findings are consistent with the much greater inhibitory effect of the GS967 on the I_{Na-L} rather than the peak transient I_{Na}[1, 4]. Aconitine prolonged the APD of cells located near the injection site from 78±8 ms to 110±12 ms and increased the maximum slope of the APD restitution curve from a baseline 1.02±0.3 to 1.44±0.5 (P<0.05). GS967 flattened the slope of the APD restitution to 0.72±0.2 at baseline, and to 0.82±0.3 after aconitine (P<0.05 for both comparisons) (Figure 7E). These effects of aconitine and GS967 on APD and APD restitution are consistent with previous reports.[2,25] GS967 had no proarrhythmic effects either during sinus rhythm or during rapid ventricular pacing (Supplemental Figure 1).

Effect of GS967 against oxidative VT/VF in the aged fibrotic hearts

We also determined the efficacy of GS967 against H_2O_2-induced arrhythmias. Oxidative stress induced by H_2O_2 is known to cause significant increases in I_{Na-L}[10, 11] and promotes EADs and triggered focal VT/VF in the aged fibrotic rat hearts.[2, 22]

Suppressive effect of GS967 against oxidative VT/VF

H_2O_2 (0.1 mM) promoted EAD-mediated VF in all eight aged hearts studied within 18 min of perfusion (Figure 8A). GS967 terminated VF within 4 min of perfusion in 5 out of 8 hearts as shown in Figure 8B (P<0.013, Exact Fisher test). Washout of GS-967 from the perfusate in the continuous presence of H_2O_2 led to the reemergence of the VF in these five hearts within 12 min, as shown in Figure 8C.

Preventive effect

In eight aged rats, 1 μM GS967 was perfused for 15 min prior to the introduction of 0.1 mM H_2O_2 in the perfusate. GS967 pretreatment prevented the emergence of VF in 5 of these 8 hearts for up to 90 min in the continuous presence of and H_2O_2 (P<0.03, Fisher Exact test). The washout of GS-967 led to the reemergence of VF in 4 of these 5 hearts.

Effects of GS967 against pacing-induced VT/in the aged hearts

In six aged hearts we studied the effect of GS967 on rapid pacing induced reentrant VF that we previously described. In all six hearts, pacing-induced reentrant VF lasted for >5 minutes consistent with our previous report[26] and were terminated by electrical shock as shown in Figure 8D. Pretreatment with GS967 fifteen min prior to rapid pacing had no effect on VF inducibility as the VF was induced in all 6 hearts as shown in Figure 8E. However, pretreatment with GS967 shortened the duration of the pacing-induced VF to less than 8 sec causing spontaneous termination of the VF (Figure 8E). The duration of the induced VF in the presence of GS-967 was significantly shorter than in its absence (6±2 sec vs. >5 min; P<0.01).

Discussion

The results of this study show that selective inhibition of the I_{Na-L} with GS967 suppresses and prevents VT/VF associated with the two stressors, aconitine[16] and H_2O_2[22]. Both stressors initiate rapid focal VT that degenerates to VF within seconds [2, 16, 18] that is maintained by multifocal activation (Figure 3) with occasional incomplete reentrant wavefronts wandering between the LV epicardial foci.[2, 18] Aconitine directly interferes with Na channel inactivation [8, 9] whereas H_2O_2[10, 11] activates Ca-calmodulin-dependent kinase II (CaMKII) to indirectly enhance I_{Na-L} as well as affect other ion channels including the L-type Ca current.[27, 28] The increase in Na loading also promotes intracellular Ca overload, which further promotes EADs, DADs and triggered activity.[12, 29] GS967 and other I_{Na-L}

inhibitors (i.e., ranolazine) have previously been shown to suppress EADs, DADs and triggered beats in isolated canine and rabbit atrial and ventricular tissues[1, 4] and in ventricular myocytes isolated from human hearts with hypertrophic cardiomyopathy.[6] Our study extends these findings on isolated myocytes to EAD- and DAD-induced VT/VF in intact isolated hearts and uses a selective $I_{Na\text{-}L}$ inhibitor to establish the role of this current in cardiac arrhythmogenesis. By blocking the $I_{Na\text{-}L,}$ GS967 suppressed the EADs and DADs that reduced the number of multiple foci to one single focus (i.e., monomorphic VT) before the sinus rhythm was restored. GS967 also shortened the APD in a use-dependent manner, reduced the spatial dispersion of repolarization and flattened the slope of the APD restitution curve, which suppressed wavebreak[30]. Because spatial dispersion of repolarization (APD) and steeper slope of APD restitution contribute to wavebreak and reentrant activation[30, 31] these effects may contribute to the suppressive effect of GS967 of mixed focal and reentrant VF.[26]

Potential Clinical Impact

Drugs that selectively block $I_{Na\text{-}L}$ could be highly effective antiarrhythmic drugs particularly against focal tachyarrhythmias. In addition, because $I_{Na\text{-}L}$ inhibition reduces spatial-temporal dispersion (Figure 6) and flattens the slope of the APD restitution curve (Figure 7), inhibition of the $I_{Na\text{-}L}$ may also be effective in suppressing reentrant form of tachyarrhythmias. Figure 9 summarizes schematically the potential antiarrhythmic spectrum of GS967. An equally important feature of $I_{Na\text{-}L}$ inhibition is that the intervention does not interfere with the normal cardiac excitation-contraction coupling and do not slow conduction. Unlike conventional antiarrhythmic drugs, no proarrhythmic effects were identified in this study that would limit the therapeutic usefulness of this class of compounds.[32–34]

Limitations

It could be argued that our 2D map may miss other mechanisms of VT/VF within the wall of the LV or on the endocardial surface. We cannot exclude the possibility that some of the triggered beats might have originated from Purkinje fibers as aconitine could have diffused from the LV injection site to the endocardium. In fact, we have seen in a few instances multiple simultaneous foci appearing on the epicardial surface with some of these perhaps reflecting breakthrough of triggered beats from Purkinje cells that become suppressed by GS967.[4] However, epicardial cells are also capable of generating EADs and triggered activity as we previously have shown in hearts with endocardial and midmyocardial ablations.[22, 35]

Supplementary Material

Refer to Web version on PubMed Central for supplementary material.

Acknowledgments

We thank Hong Cao, MD, for preparing the manuscript.

This study was supported by NIH Grants P01 HL079831, the Laubisch Endowments and a research grant from Gilead Sciences Inc., Foster City California

Abbreviations

APD	action potential duration
APA	action potential amplitude

CL	cycle length
EAD	early afterdepolarizations
DAD	delayed afterdepolarizations
H_2O_2	hydrogen peroxide
IC_{50}	concentration for 50% inhibition
$I_{Na\text{-}L}$	late inward Na current
IKr	delayed rectified potassium current
VT	ventricular tachycardia
VF	ventricular fibrillation

References

1. Belardinelli L, Liu G, Smith-Maxwell C, et al. A Novel, Potent, and Selective Inhibitor of Cardiac Late Sodium Current Suppresses Experimental Arrhythmias. J Pharmacol Exp Ther. 2012
2. Morita N, Lee JH, Xie Y, et al. Suppression of re-entrant and multifocal ventricular fibrillation by the late sodium current blocker ranolazine. J Am Coll Cardiol. 2011; 57(3):366–375. [PubMed: 21232675]
3. Dhalla AK, Wang WQ, Dow J, et al. Ranolazine, an antianginal agent, markedly reduces ventricular arrhythmias induced by ischemia and ischemia-reperfusion. Am J Physiol Heart Circ Physiol. 2009; 297(5):H1923–1929. [PubMed: 19767532]
4. Sicouri S, Belardinelli L, Antzelevitch C. Antiarrhythmic effects of the highly selective late sodium channel current blocker GS-458967. Heart Rhythm. 2013; 10:1036–1043. [PubMed: 23524321]
5. Maltsev VA, Undrovinas A. Late sodium current in failing heart: friend or foe? Prog Biophys Mol Biol. 2008; 96(1–3):421–451. [PubMed: 17854868]
6. Coppini R, Ferrantini C, Yao L, et al. Late sodium current inhibition reverses electromechanical dysfunction in human hypertrophic cardiomyopathy. Circulation. 2013; 127(5):575–584. [PubMed: 23271797]
7. Bennett PB, Yazawa K, Makita N, et al. Molecular mechanism for an inherited cardiac arrhythmia. Nature. 1995; 376(6542):683–685. [PubMed: 7651517]
8. Peper K, Trautwein W. The effect of aconitine on the membrane current in cardiac muscle. Pflugers Arch Gesamte Physiol Menschen Tiere. 1967; 296(4):328–336.
9. Nilius B, Boldt W, Benndorf K. Properties of aconitine-modified sodium channels in single cells of mouse ventricular myocardium. Gen Physiol Biophys. 1986; 5(5):473–484. [PubMed: 2433183]
10. Song Y, Shryock JC, Wagner S, et al. Blocking late sodium current reduces hydrogen peroxide-induced arrhythmogenic activity and contractile dysfunction. J Pharmacol Exp Ther. 2006; 318(1): 214–222. [PubMed: 16565163]
11. Ward CA, Giles WR. Ionic mechanism of the effects of hydrogen peroxide in rat ventricular myocytes. Journal of Physiology. 1997; 500 (Pt 3):631–642. [PubMed: 9161981]
12. Shryock JC, Song Y, Rajamani S, et al. The Arrhythmogenic Consequences of Increasing Late INa in the Cardiomyocyte. Cardiovasc Res. 2013
13. Sawanobori T, Hirano Y, Hiraoka M. Aconitine-induced delayed afterdepolarization in frog atrium and guinea pig papillary muscles in the presence of low concentrations of Ca2+ Jpn J Physiol. 1987; 37:59–79. [PubMed: 3497297]
14. Amran MS, Hashimoto K, Homma N. Effects of sodium-calcium exchange inhibitors, KB-R7943 and SEA0400, on aconitine-induced arrhythmias in guinea pigs in vivo, in vitro, and in computer simulation studies. J Pharmacol Exp Ther. 2004; 310(1):83–89. [PubMed: 15028781]
15. Scherf D. Studies on auricular tachycardia caused by aconitine administration. Proc Exp Biol Med. 1947; 64:233–239.

16. Swissa M, Qu Z, Ohara T, et al. Action potential duration restitution and ventricular fibrillation due to rapid focal excitation. Am J Physiol Heart Circ Physiol. 2002; 282(5):H1915–H1923. [PubMed: 11959659]
17. Adaniya H, Hayami H, Hiraoka M, et al. Effects of magnesium on polymorphic ventricular tachycardias induced by aconitine. J Cardiovasc Pharmacol. 1994; 24(5):721–729. [PubMed: 7532749]
18. Sato D, Xie LH, Sovari AA, et al. Synchronization of chaotic early afterdepolarizations in the genesis of cardiac arrhythmias. Proc Natl Acad Sci US A. 2009; 106(9):2983–2988.
19. Antzelevitch C, Burashnikov A, Sicouri S, et al. Electrophysiologic basis for the antiarrhythmic actions of ranolazine. Heart Rhythm. 2011; 8(8):1281–1290. [PubMed: 21421082]
20. Smith-Maxwell CJ, Xie C, Chan K, et al. Discovery of GS-485967: a novel and highly selective inhibitor of cardiac sodium late current. Heart Rhythm. 2012; 9:S394.
21. Pezhouman A, Madahian S, Stepanyan H, et al. Selective Inhibition of the Late Sodium Current to Prevent Ventricular Fibrillation. Circulation. 2013
22. Morita N, Sovari AA, Xie Y, et al. Increased Susceptibility of Aged Hearts to Ventricular Fibrillation During Oxidative Stress. Am J Physiol Heart Circ Physiol. 2009; 297:H1594–H1605. [PubMed: 19767530]
23. Bapat A, Nguyen TP, Lee JH, et al. Enhanced Sensitivity of Aged Fibrotic Hearts to Angiotensin II- & Hypokalemia-Induced Early Afterdepolarizations-Mediated Ventricular Arrhythmias. Am J Physiol Heart Circ Physiol. 2012; 302:H2331–H2340. [PubMed: 22467308]
24. Xie LH, Chen F, Karagueuzian HS, et al. Oxidative Stress-Induced Afterdepolarizations and Calmodulin Kinase II Signaling. Circulation Research. 2009; 104:79–86. [PubMed: 19038865]
25. Jung BC, Lee SH, Cho YK, et al. Role of the alternans of action potential duration and aconitine-induced arrhythmias in isolated rabbit hearts. J Korean Med Sci. 2011; 26(12):1576–1581. [PubMed: 22147994]
26. Hayashi H, Wang C, Miyauchi Y, et al. Aging-related increase to inducible atrial fibrillation in the rat model. Journal of Cardiovascular Electrophysiology. 2002; 13(8):801–808. [PubMed: 12212701]
27. Wagner S, Dybkova N, Rasenack EC, et al. Ca2+/calmodulin-dependent protein kinase II regulates cardiac Na+ channels. J Clin Invest. 2006; 116(12):3127–3138. [PubMed: 17124532]
28. Erickson JR, He BJ, Grumbach IM, et al. CaMKII in the Cardiovascular System: Sensing Redox States. Physiol Rev. 2011; 91(3):889–915. [PubMed: 21742790]
29. Qu Z, Xie LH, Olcese R, Karagueuzian HS, et al. Early Afterdepolarizations in Cardiac Myocytes: Beyond Reduced Repolarization Reserve. Cardiovasc Res. 2013; 99:6–15. [PubMed: 23619423]
30. Weiss JN, Chen PS, Qu Z, et al. Ventricular fibrillation : how do we stop the waves from breaking? Circulation Research. 2000; 87:1103–1107. [PubMed: 11110766]
31. Swissa M, Qu Z, Ohara T, et al. Action potential duration restitution and ventricular fibrillation due to rapid focal excitation. Pacing Clin Electrophysiol. 2001; 24(II):713.
32. Morganroth J, Goin JE. Quinidine-related mortality in the short-to medium-term treatment of ventricular arrhythmias. Circulation. 1991; 84(1):1977–1983. [PubMed: 1834365]
33. Karagueuzian, HS.; JMW. Antiarrhythmic Drugs: Mode of Action, Pharmacokinetic Properties, and Therapeutic Uses. 3. Philadelphia: J.B. Lippincott Company; 1995.
34. Farkas A, Lepran I, Papp JG. Proarrhythmic effects of intravenous quinidine, amiodarone, D-sotalol, and almokalant in the anesthetized rabbit model of torsade de pointes. J Cardiovasc Pharmacol. 2002; 39(2):287–297. [PubMed: 11791015]
35. Morita N, Lee JH, Bapat A, et al. Glycolytic Inhibition Causes Spontaneous Ventricular Fibrillation in Aged Hearts. Am J Physiol Heart Circ Physiol. 2011; 301:H180–H191. [PubMed: 21478408]

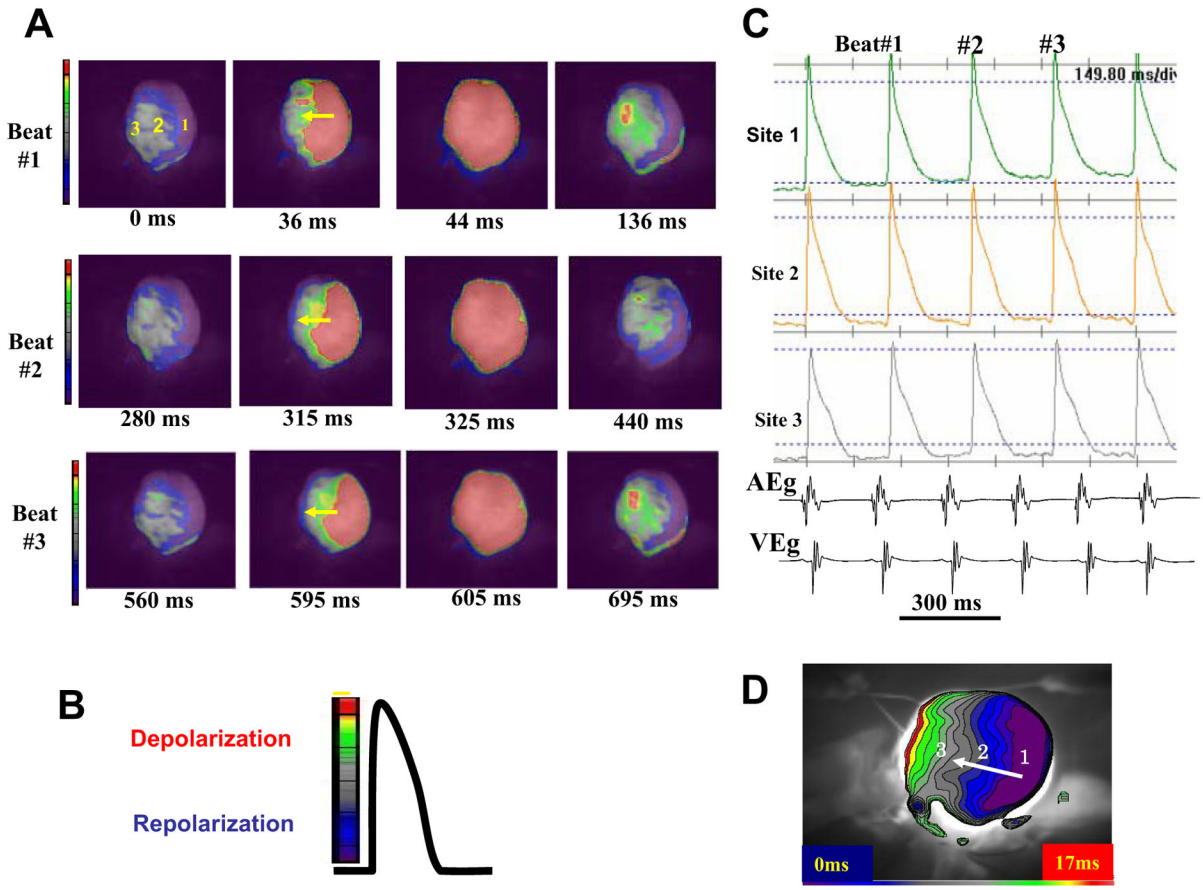

Figure 1. Optical snap shots, action potentials and isochronal activation map during sinus rhythm in an adult rat heart

Panel A shows three consecutive sinus beats (Beats # 1 to #3), with red indicating depolarization and blue/purple repolarization as shown in panel B. The yellow arrows indicate the direction of wave propagation. Panel C shows selected action potentials recorded from sites 1, 2, and 3 indicated in panel A. Panel D is an isochronal map with blue indicating time zero. Notice that no conduction block is present.

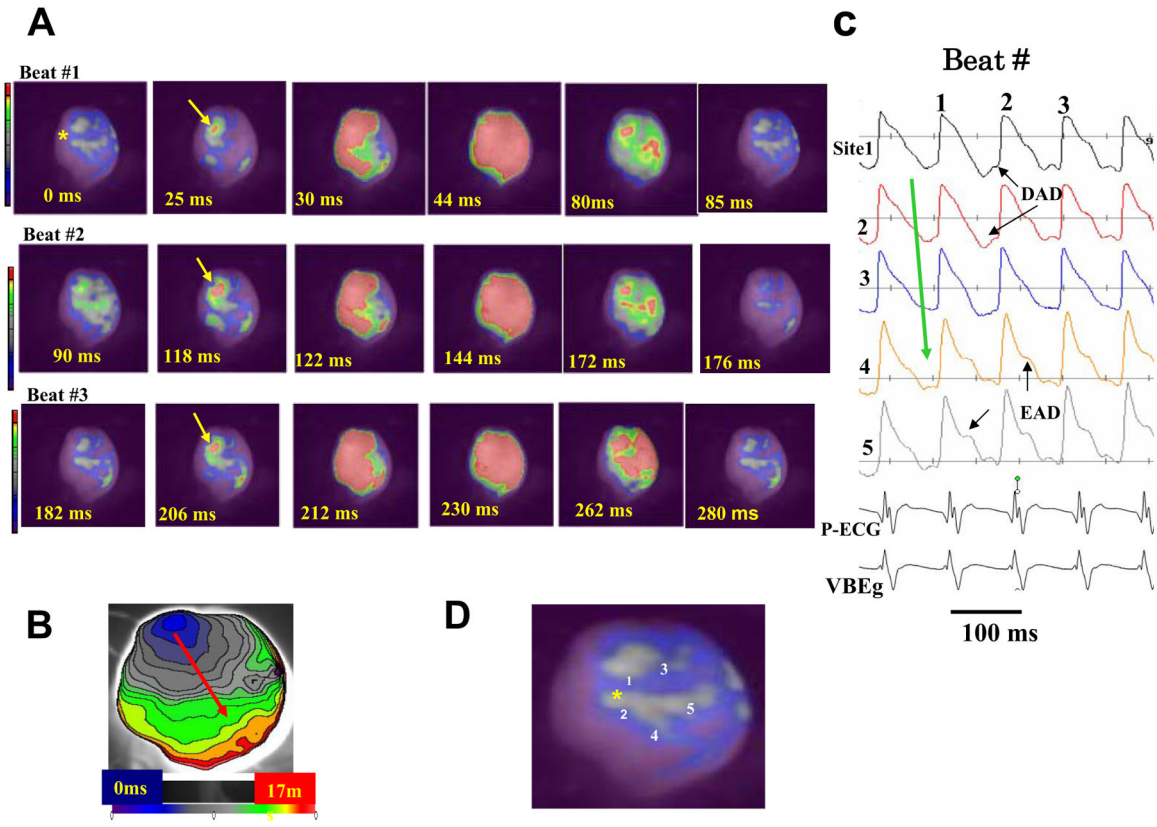

Figure 2. Optical snap shots (A), isochronal activation map (B) and selected action potentials (C) recorded at the onset of a focal monomorphic VT induced after local injection of aconitine

The site of aconitine injection is shown by a yellow asterisk in the snap shot arbitrarily labeled as time 0 ms in panel A (beat #1). A focal activity arises 25 ms later located near the site of aconitine injection (yellow arrow) that propagates (red arrow shows the direction of wave propagation) without block within 17 ms as shown in the isochronal activation map in panel B. Immediately after the recovery of the first VT beat (90 ms), a second focal activity arises 118 ms later from the same site (beat #2) which propagates as in beat #1, then a third beat (beat #3) arises again from the same focal site and propagating as the previous two beats. Panel C shows optical action potentials recorded from near the aconitine injection sites (yellow asterisk) with the suggested presence of DADs and EADs during the focal VT. Panel D shows the heart silhouette with the sites of optical APs recordings shown in panel C.

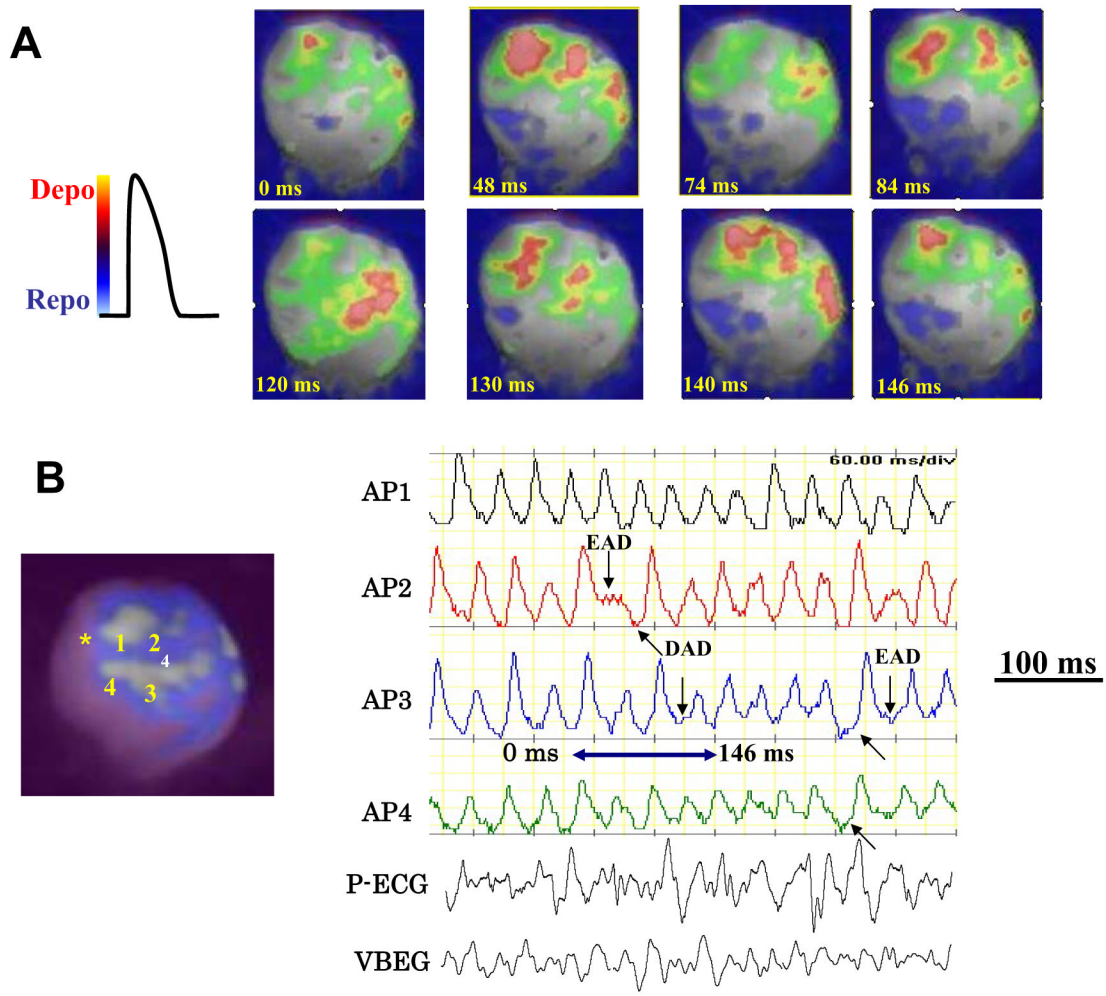

Figure 3. Optical snap shots and selected action potentials during aconitine-induced VF

The snap shots in panel A show multiple activation foci (red color) separated by recovered tissue that arise from both near the aconitine injection site (yellow asterisk in panel B) and also from the mid LV regions. Panel B shows selected action potentials from sites indicated in the adjoining heart silhouette providing hints of EADs (downward arrows) and DADs (upward arrows). The blue double-headed arrow indicates the period of the VF during which the snap shots are shown in panel A.

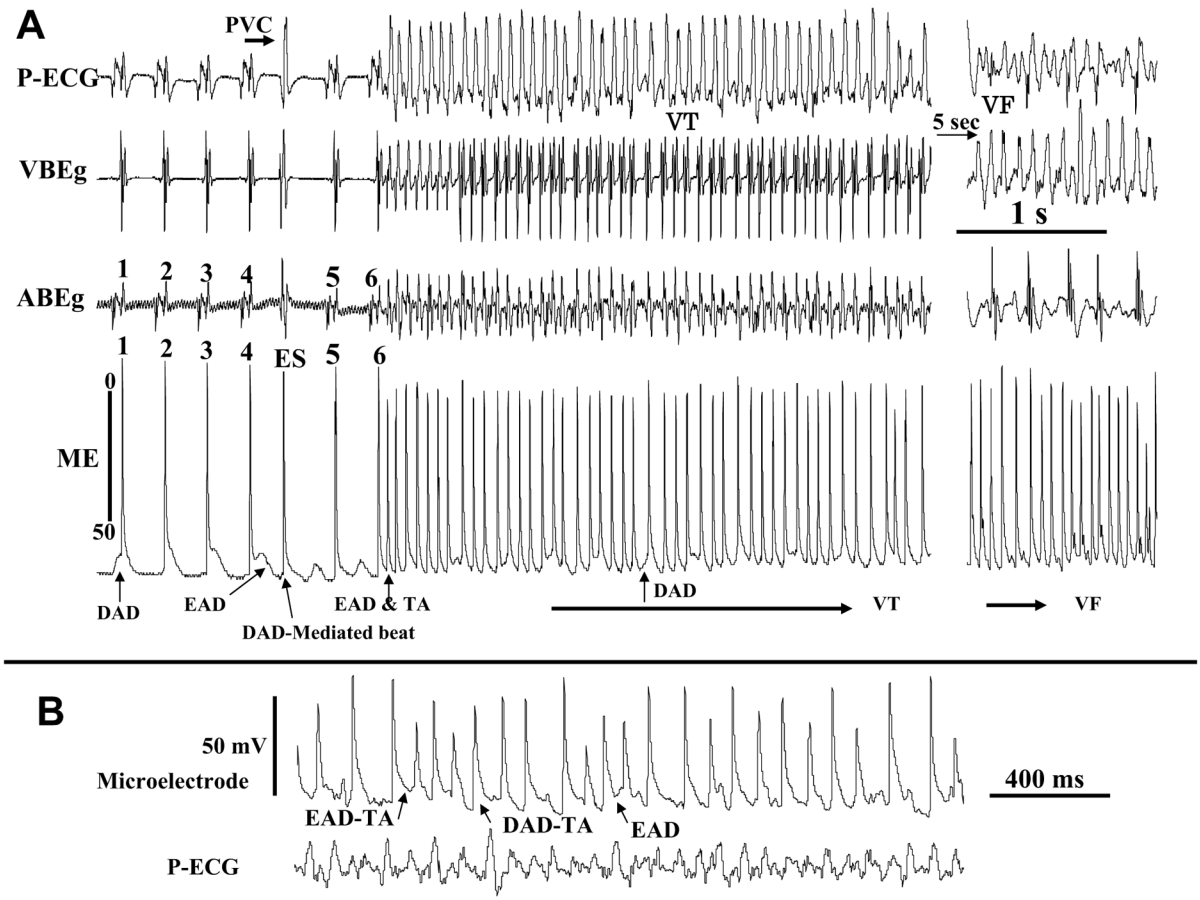

Figure 4. Simultaneous microelectrode and electrocardiograms recorded during aconitine-induced transition from sinus rhythm to monomorphic VT then VF

Shown in panel A are the last six beats of sinus origin showing cellular EADs and DADs captured with the microelectrode recording (arrows). Notice a single DAD-mediated triggered ventricular beat (ES, extrasystole) between sinus beats 4 and 5. The AP upstroke of the DAD-induced triggered beat precedes by 8 ms the QRS of the simultaneously recorded ECG, indicating that the triggered beat is the source of the ES seen on the ECG. Notice also that the DADs often arise following a previous AP with an EAD, presumably because the prolonged APD allows overloading the SR with Ca so to promote spontaneous Ca_i^{2+} waves causing DAD-mediated triggered activity. Panel B shows faster sweep speed during VF to make each of the EAD and the DAD mechanisms more visible.

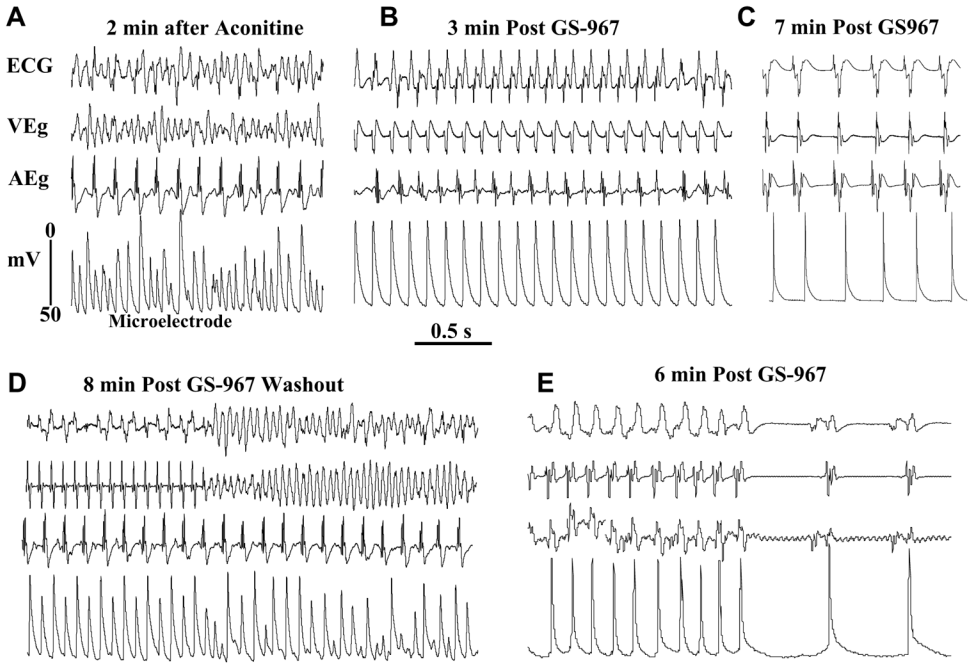

Figure 5. Suppression of aconitine-induced VT/VF with GS967 (1 μM) and reversal of its effect upon washout

Panel A shows aconitine-induced VF which converts to monomorphic VT 3 min after arterial perfusion of GS967 (panel B) and to sinus rhythm 7 min after GS967 (panel C). Washout of GS967 with drug-free Tyrode's perfusion causes the reemergence of monomorphic VT that degenerate to VF 8 min after GS967 washout (pane D). The reintroduction of GS967 in the perfusate suppresses the VF by first converting it to VT and then to sinus rhythm as shown in panel E. Notice the marked shortening of the APD after GS967-induced conversion of the monomorphic VT to sinus rhythm despite the lengthening of the cycle length (panels C & E).

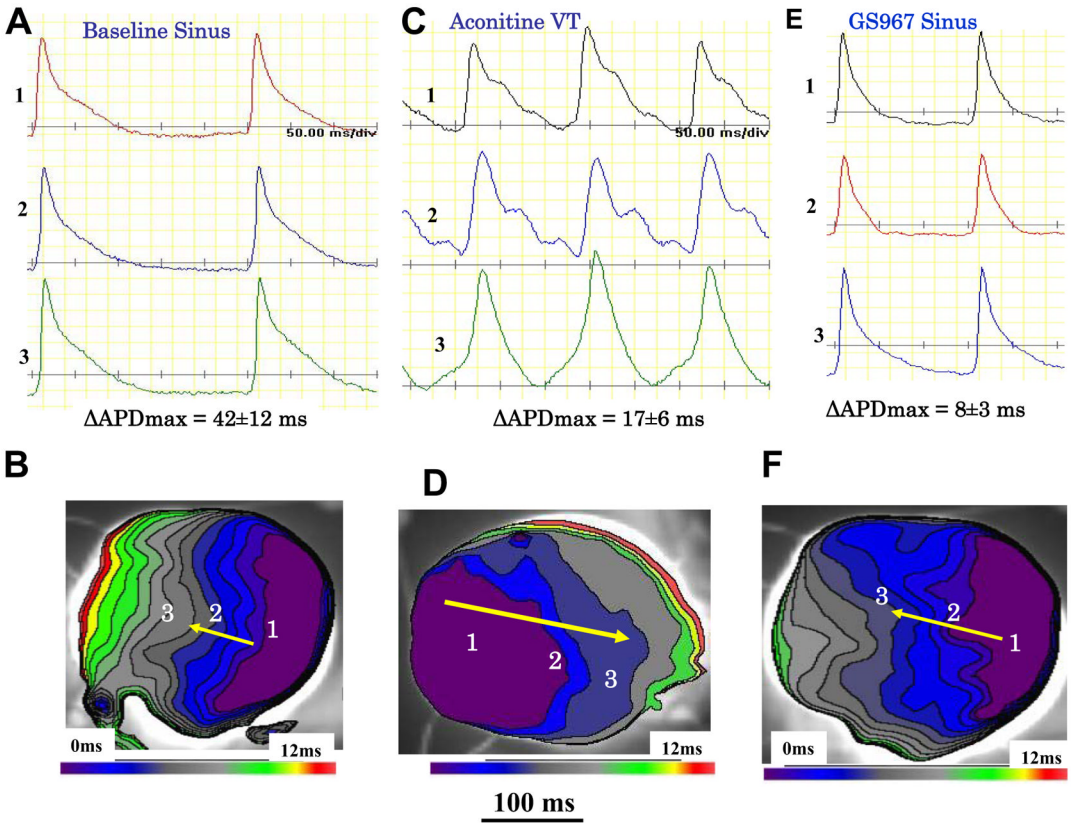

Figure 6. Reduction of spatial action potential duration (APD) dispersion over the LV epicardial surface caused by GS967 perfusion

Panel A shows baseline optical AP recordings from sites 1 to 3 shown in the isochronal activation map in panel B. The maximum APD difference (longest APD minus shortest APD) averaged 42±12 ms at baseline. During aconitine-induced VT the maximum APD dispersion decreased to 17±6 ms (panel C) without affecting conduction time (panel D). Perfusion with GS967 shortened the APD throughout the entire LV epicardial surface and reduced the APD dispersion to 8±3 ms (panel E) without affecting conduction time (panel F).

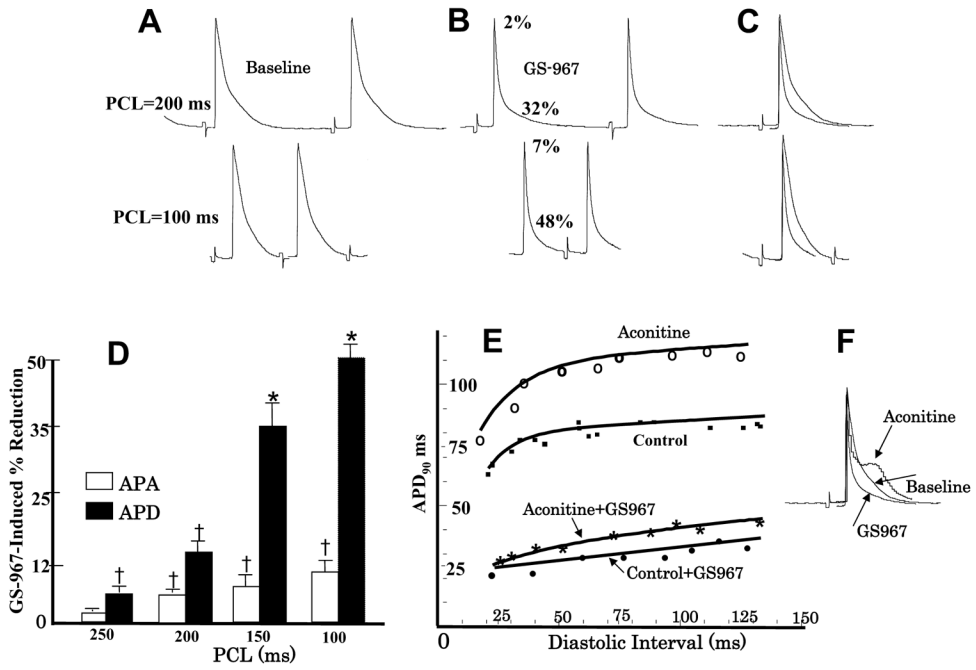

Figure 7. Effect of GS967 on use-dependent APD, action potential amplitude (APA) and APD restitution

Panel A shows baseline microelectrode recordings of action potentials at two pacing cycle lengths (PCLs), 200 ms (top) and 100 ms (bottom). Panel B shows the effects of GS967 at these two PCLs, causing 2% and 7% reduction in APA and 32% and 48% reduction in APD respectively. Panel C is superimposed APs showing that GS967 causes greater shortening of the APD than the APA at faster rates (use-dependent) and panel D is mean percent shortening of APA and APD as a function of PCL (N=6). Panel E shows the effect of GS967 on the slope of the dynamic APD restitution curves both at baseline and after aconitine. Panel F is superimposed APs at baseline, after aconitine injection just prior to the initiation of VT/VF and after GS967.

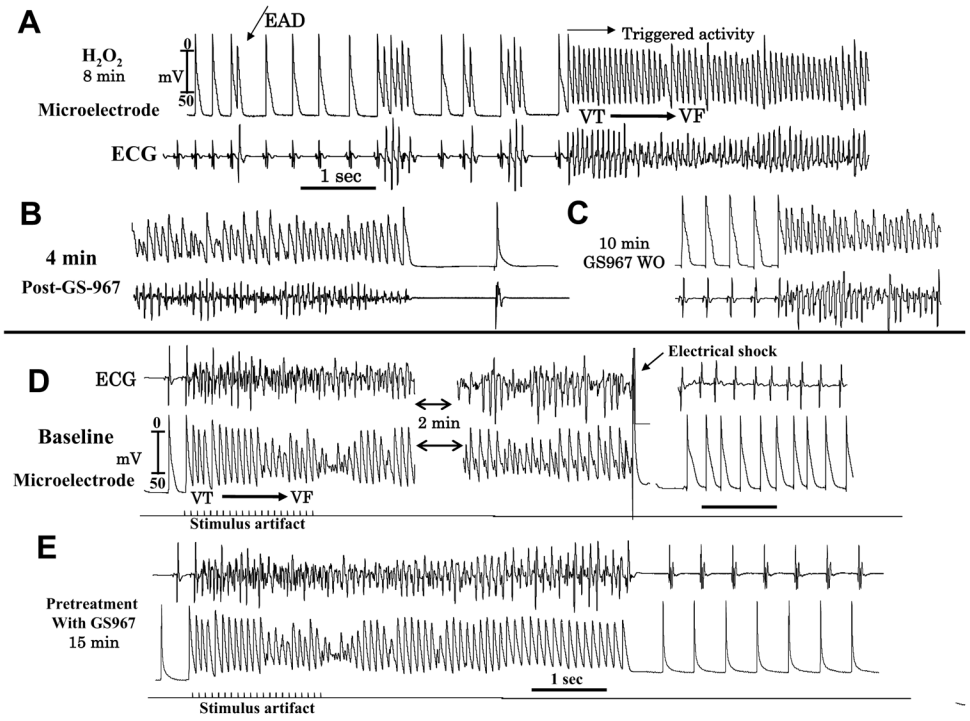

Figure 8. GS967suppresses H_2O_2-induced (hydrogen peroxide, 0.1 mM) EADs, VT/VF and prevents maintenance of pacing-induced VF in an aged heart

Panel A shows the emergence of EADs, short runs of triggered activity leading to VF at 8 min after H_2O_2 perfusion. Panel B shows suppression of the VF at 4 min after GS967 perfusion and restoration of sinus rhythm with shortening of the APD. Panel C shows the reemergence of VF at 10 min after washout of GS967. Rapid pacing induces VT/VF in the absence of H_2O_2 (Panel D) requiring electrical shock for termination. Perfusion of GS967 at 15 min prior to rapid pacing while initiating the VF (Panel E) does not sustain and terminates within 3 sec (panel E).

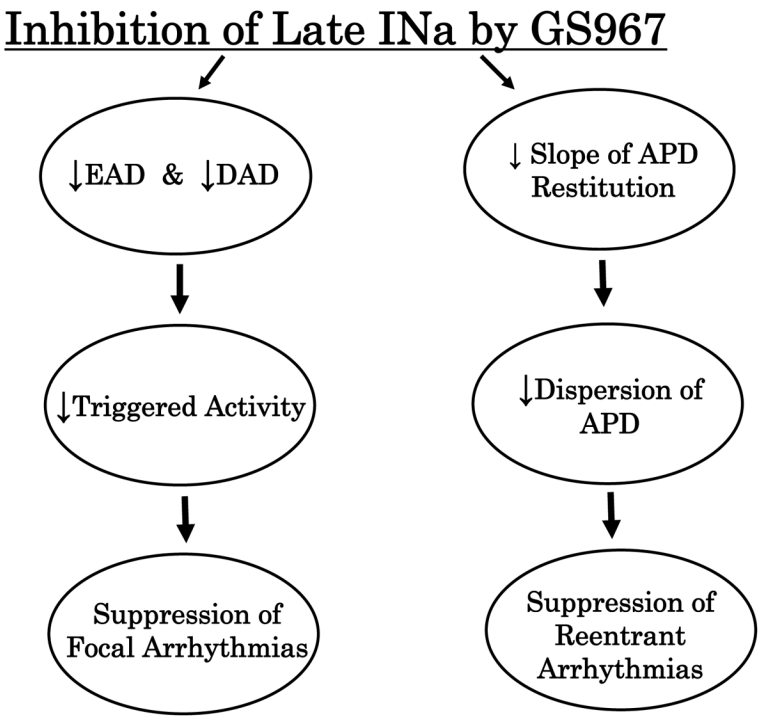

Figure 9. Schematic drawing of the effects of GS967-induced inhibition of INa-L on afterpotentials and arrhythmias

The downward pointing arrows within the ellipses indicate inhibition. All abbreviations are as indicated in the text.

Table

IC50 of Drugs for Peak INa, Late INa & IKr

Drug	Peak INa	Late INa	IKr
Flecainide	84±4 μM	3.4±0.5 μM	1.5±0.1 μM
Ranolazine	1329±114 μM	17±1 μM	13±1 μM
GS967	7.5% at 10 μM	0.13±0.01 μM	17% at 10 μM

Notice that the inhibitory effect of GS967 on peak INa and IKr becomes manifest only at 10 μM (i.e., 10 times higher than the concentration used in this study). Numbers are mean±SEM.